Available online at www.sciencedirect.com
ScienceDirect
Scripta Materialia 99 (2015) 49–52
Scripta MATERIALIA
www.elsevier.com/locate/scriptamat

Designing Fe–Mn–Si alloys with improved low-cycle fatigue lives

Takahiro Sawaguchi,[a,*] Ilya Nikulin,[a] Kazuyuki Ogawa,[a] Kaoru Sekido,[a] Susumu Takamori,[a] Tadakatsu Maruyama,[b] Yuya Chiba,[b] Atsumichi Kushibe,[c] Yasuhiko Inoue[c] and Kaneaki Tsuzaki[a,d]

[a] *National Institute for Materials Science, 1-2-1 Sengen, Tsukuba, Ibaraki 305-0047, Japan*
[b] *Awaji Materia Co.Ltd., 2-3-13, Kanda Ogawamachi, Chiyoda, Tokyo 101-0052, Japan*
[c] *Takenaka Corporation, 1-5-1, Otsuka, Inzai, Chiba 270-1395, Japan*
[d] *Kyushu University, 744 Motooka, Nishi-ku Fukuoka, 819-0395, Japan*

Received 18 September 2014; revised 14 November 2014; accepted 17 November 2014
Available online 8 December 2014

A new design concept for improving the low-cycle fatigue lives of Fe–Mn–Si-based alloys is proposed. The degree of reversibility of the dislocation motion can be increased by setting the stacking fault energy to approximately 20 mJ m^{-2}, enhancing the Ni-equivalent amounts with respect to the Cr-equivalent amounts and setting the Si concentration to 4 wt.%. Under these conditions, an Fe–15Mn–10Cr–8Ni–4Si alloy with a low-cycle fatigue life of approximately 8000 cycles for a total strain range of 2.0% could be developed.

Keywords: Shape memory alloys (SMA); Fe–Mn–Si; Fatigue; Damping; Martensitic phase transformation

Fe–Mn–Si-based alloys are known to show a shape-memory effect associated with the deformation-induced martensitic transformation from face-centred cubic γ-austenite to hexagonal close-packed ε-martensite on loading and its reversion on subsequent heating [1]. Apart from being employed in other applications, these alloys are used for the fish plates of coupling crane rails at industrial sites [2]. In terms of mechanical properties, Fe–Mn–Si-based alloys are low-stacking-fault-energy (SFE) high–Mn austenitic steels, which are being studied intensively as the next-generation structural steels [3]. They exhibit superior mechanical properties owing to characteristic plasticity mechanisms such as mechanical γ-twinning and a deformation-induced γ→ε martensitic transformation; these phenomena are called twinning- and transformation-induced plasticity (TWIP/TRIP) effects, respectively. Consequently, Fe–Mn–Si-based alloys are capable of being used as structural alloys that exhibit the shape-memory functionality [4].

Recently, Sawaguchi et al. [5] proposed that Fe–Mn–Si-based alloys can be used for the seismic damping of architectural constructions. Seismic metallic dampers absorb the vibrations of buildings through elastoplastic deformation; however, severe deformations cause fatigue in the damper metal. An Fe–Mn–Si-based alloy with the chemical composition of Fe–28Mn–5Cr–6Si–0.5NbC (in wt.%) was reported to exhibit a stable damping capacity associated with reversible martensitic transformations under cyclic push–pull loading [6]. This stable deformation behaviour with enhanced fatigue properties makes such alloys highly suited for use in seismic dampers, in particular against long-duration ground motion. For this purpose, we attempted to develop new Fe–Mn–Si-based alloys with enhanced low-cycle fatigue (LCF) lives, N_f.

The central idea behind the design concept is the reversibility of the plasticity mechanisms characteristic of low-SFE alloys. Figure 1 illustrates schematic models of the reversible dislocation motions associated with (a, b) a deformation-induced γ→ε martensitic transformation, (c, d) deformation γ-twinning and (e, f) extended dislocation gliding [7]. These plasticity mechanisms commonly originate from the regularly or irregularly integrated movement of Shockley partials as they leave stacking faults. Owing to the geometric restrictions of the cross-slip of the partial-fault unit, their movement is confined on a unique {111} plane of the γ-crystal. It is known that extended dislocation gliding results in planar dislocation arrangements, and not the typical dislocation cell structures; the former are beneficial for improving the LCF properties [8]. Chalant and Remy [9] found that Co–Ni alloys showing ε-martensite and γ-twins also exhibit an improved N_f. These may have the same origin, that is to say, they might be caused by the reversible movement of Shockley partials on an identical {111} plane. The reversible movement of Shockley partials in the case of (b) accompanies the reverse ε→γ martensitic transformation that was experimentally observed in our previous study [5]. It is therefore speculated that case (d) should exhibit detwinning.

* Corresponding author.

http://dx.doi.org/10.1016/j.scriptamat.2014.11.024
1359-6462/

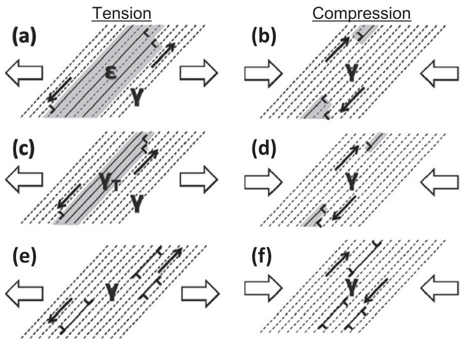

Figure 1. Schematic diagrams of the reversible group motion of the dislocations in (a, c, e) tension and (b, d, f) compression. (a, b) Deformation-induced ε-martensitic transformation, (c, d) mechanical γ-twinning, (e, f) extended dislocation gliding. The dashed and solid lines represent {111} planes of the γ-crystal and stacking faults, respectively.

In order to determine the optimal alloy composition, we investigated the LCF properties in binary Fe–*x*Mn ($x = 5$ to 40) alloys, in ternary Fe–33Mn–*y*Si ($y = 0$ to 6) alloys, in quaternary Fe–30Mn–*z*Si–(6 – *z*)Al ($z = 0$ to 6) alloys, and in quinary Fe–15Mn–10Cr–8Ni–*s*Si ($s = 0$ to 6) alloys (the chemical compositions are shown in wt.%, unless otherwise stated). The alloy compositions in the former three alloy systems were selected to cover sufficiently wide SFE ranges, and include some typical SMAs ($y = 6$ and $z = 6$) and TWIP/TRIP steels ($z = 3$ and 4) reported in the literature [1,3,10–12], while those in the Fe–Mn–Cr–Ni–Si system were determined according to the design criteria established in the present work, which will be described later. We have recently reported that the Fe–Mn–Si–Al alloys have superior LCF properties than conventional steels, and N_f >8000 at the total strain range of 2.0% is obtained in the alloy with $z = 4$ [10]. The present article is devoted to surveying the LCF properties across the four alloy systems to draw design criteria for improving N_f.

The alloys were prepared by induction furnace melting and formed into 10 kg ingots. They were hot forged and rolled after preheating at 1273 K, then solutionized at 1273 K for 1 h in an Ar atmosphere and subsequently quenched in water. Cylindrical LCF specimens with a diameter of 8 mm were machined from the ingots, and their surface was mechanically ground in successive stages by SiC down to a 600 grid of the JIS standard. They were then subjected to axial-strain-controlled LCF tests in air at a constant total strain of 2.0% with a constant strain rate of $4 \cdot 10^{-3}\ s^{-1}$ until they underwent fatigue fracturing. The chemical compositions, the LCF lives, N_f, the stress amplitudes and the hysteresis energies at $N_f/2$, $\Delta\sigma/2_{Nf/2}$ and $\Delta W_{Nf/2}$, respectively, are listed in Table 1. Measurements were repeated for alloys of particular interest, whereas the data for other alloys represent single measurements. In the case of the former, error bars and standard deviations for the N_f values are shown in Figure 2 and Table 1. The volume fractions of the constituent phases were determined using X-ray diffraction analyses, and the deformation microstructures were observed using scanning electron microscopy–electron backscatter diffraction (SEM–EBSD) and transmission electron microscopy (TEM).

Figure 2(a)–(d) demonstrates the composition dependence of N_f; the previously reported values [13] for the

Table 1. Chemical compositions, the number of cycles to fatigue fracture, N_f, the stress amplitude and the hysteresis energy at $N_f/2$, $\Delta\sigma/2_{Nf/2}$ and $\Delta W_{Nf/2}$, respectively.

No.	Chemical composition	N_f (cycles)	$\Delta\sigma/2_{Nf/2}$ (MPa)	$\Delta W_{Nf/2}$ (MN/m^2)
Fe-xMn				
$x = 5$	Fe-4.95Mn	278	458	1189
$x = 10$	Fe-9.77Mn	294	586	1364
$x = 15$	Fe-14.9Mn	426	668	1318
$x = 20$	Fe-19.8Mn	684	607	874
$x = 25$	Fe-24.0Mn	1620	574	838
$x = 30$	Fe-28.4Mn	994	470	896
$x = 35$	Fe-32.3Mn	884	396	1033
$x = 40$	Fe-39.7Mn	287	382	1043
Fe-33Mn-ySi				
$y = 0$	Fe-33.3Mn	917	370	990
$y = 2$	Fe-33.2Mn-1.9Si	2318	403	907
$y = 4$	Fe-33.9Mn-3.9Si	3162	460	885
$y = 6$	Fe-32.5Mn-6.1Si	2833	492	908
Fe-30Mn-zSi-(6-z)Al				
$z = 0$	Fe-30.0Mn-5.8Al	750	389	969
$z = 1$	Fe-29.9Mn-1.0Si-5.25Al	770	398	981
$z = 2$	Fe-30.5Mn-2.0Si-4.1Al	1790	403	972
$z = 3$	Fe-29.9Mn-3.0Si-3.0Al	2112	396	937
$z = 4$	Fe-30.0Mn-4.1Si-2.0Al	8374 ± 873	392	731
$z = 5$	Fe-30.1Mn-5.0Si-0.97Al	2080	455	871
$z = 6$	Fe-30.1Mn-6.1Si	2024	450	884
Fe-15Mn-10Cr-8Ni-sSi				
$s = 0$	Fe-14.9Mn-10.3Cr-8.1Ni	2858	340	773
$s = 2$	Fe-15.0Mn-10.4Cr-8.1Ni-1.7Si	3205	366	834
$s = 4$	Fe-15.1Mn-10.4Cr-8.1Ni-3.6Si	8466 ± 1439	385	743
$s = 6$	Fe-15.0Mn-10.3Cr-8.1Ni-5.6Si	4451	412	800